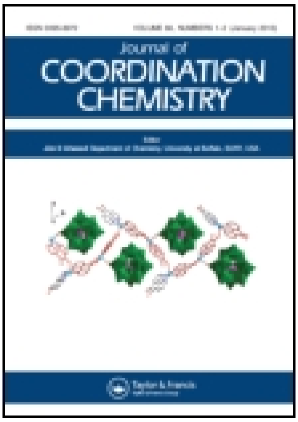

Journal of Coordination Chemistry
Publication details, including instructions for authors and subscription information:
http://www.tandfonline.com/loi/gcoo20

Synthesis, characterization, and thermal behavior of Cu(II) and Zn(II) complexes with (E)-2-[N′-(1-pyridin-2-yl-ethylidene)hydrazino]acetic acid (aphaOH). Crystal structure of [$Zn_2(aphaO)_2Cl_2$]

Nenad Filipović [a] , Marija Borna [b] , Olivera Klisurić [c] , Matej Pregelj [d] , Marko Jagodič [e] [f] , Katarina Anđelković [g] & Tamara Todorović [g]

[a] Faculty of Agriculture , University of Belgrade , Belgrade , Republic of Serbia
[b] Max Planck Institute for Chemical Physics of Solids , Dresden , Germany; Computer-Chemistry-Center, Friedrich-Alexander-Universität Erlangen-Nürnberg, Erlangen, Germany
[c] Faculty of Sciences , University of Novi Sad , Novi Sad , Republic of Serbia
[d] Jožef Stefan Institute , Ljubljana , Slovenia
[e] Institute of Mathematics, Physics and Mechanics , Ljubljana , Slovenia
[f] EN-FIST Centre of Excellence , Ljubljana , Slovenia
[g] Faculty of Chemistry , University of Belgrade , Belgrade , Republic of Serbia

To cite this article: Nenad Filipović , Marija Borna , Olivera Klisurić , Matej Pregelj , Marko Jagodič , Katarina Anđelković & Tamara Todorović (2013) Synthesis, characterization, and thermal behavior of Cu(II) and Zn(II) complexes with (E)-2-[N′-(1-pyridin-2-yl-ethylidene)hydrazino]acetic acid (aphaOH). Crystal structure of [$Zn_2(aphaO)_2Cl_2$], Journal of Coordination Chemistry, 66:9, 1549-1560, DOI: 10.1080/00958972.2013.786052

To link to this article: http://dx.doi.org/10.1080/00958972.2013.786052

PLEASE SCROLL DOWN FOR ARTICLE

Taylor & Francis makes every effort to ensure the accuracy of all the information (the "Content") contained in the publications on our platform. However, Taylor & Francis, our agents, and our licensors make no representations or warranties whatsoever as to the accuracy, completeness, or suitability for any purpose of the Content. Any opinions and views expressed in this publication are the opinions and views of the authors, and are not the views of or endorsed by Taylor & Francis. The accuracy of the Content should not be relied upon and should be independently verified with primary sources of information. Taylor and Francis shall not be liable for any losses, actions, claims, proceedings, demands, costs, expenses, damages, and other liabilities whatsoever or howsoever caused arising directly or indirectly in connection with, in relation to or arising out of the use of the Content.

This article may be used for research, teaching, and private study purposes. Any substantial or systematic reproduction, redistribution, reselling, loan, sub-licensing, systematic supply, or distribution in any form to anyone is expressly forbidden. Terms & Conditions of access and use can be found at http://www.tandfonline.com/page/terms-and-conditions

Downloaded by [Renmin University of China] at 10:53 13 October 2013

Journal of Coordination Chemistry, 2013
Vol. 66, No. 9, 1549–1560, http://dx.doi.org/10.1080/00958972.2013.786052

Synthesis, characterization, and thermal behavior of Cu(II) and Zn(II) complexes with (*E*)-2-[*N′*-(1-pyridin-2-yl-ethylidene)hydrazino]acetic acid (aphaOH). Crystal structure of [$Zn_2(aphaO)_2Cl_2$]

NENAD FILIPOVIƆ, MARIJA BORNA‡, OLIVERA KLISURIƧ, MATEJ PREGELJ¶, MARKO JAGODIČ||,††, KATARINA ANĐELKOVIƇ‡ and TAMARA TODOROVIƇ*‡‡

†Faculty of Agriculture, University of Belgrade, Belgrade, Republic of Serbia
‡Max Planck Institute for Chemical Physics of Solids, Dresden, Germany; Computer-Chemistry-Center, Friedrich-Alexander-Universität Erlangen-Nürnberg, Erlangen, Germany
§Faculty of Sciences, University of Novi Sad, Novi Sad, Republic of Serbia
¶Jožef Stefan Institute, Ljubljana, Slovenia
||Institute of Mathematics, Physics and Mechanics, Ljubljana, Slovenia
††EN-FIST Centre of Excellence, Ljubljana, Slovenia
‡‡Faculty of Chemistry, University of Belgrade, Belgrade, Republic of Serbia

(*Received 29 June 2012; in final form 10 January 2013*)

Copper(II) and zinc(II) complexes with the condensation derivative of 2-acetylpyridine and hydrolyzed ethyl hydrazinoacetate were synthesized in a one pot reaction. Crystal structure of the zinc(II) complex was determined by single-crystal X-ray diffraction. In this binuclear complex, the ligand is coordinated via pyridine and imine nitrogen, while carboxylate oxygen is a bridge between metal centers. The fifth coordination site is occupied by a chloride, giving a distorted square pyramidal geometry around each zinc(II). The molecular structure of the copper(II) complex was determined from elemental analysis, infrared and electron paramagnetic resonance spectroscopy, molar conductivity, mass spectrometry, and measurements of the magnetic moment. Thermal behavior of both complexes was studied by thermogravimetric analysis coupled with mass spectrometer.

Keywords: Copper(II); Zinc(II); X-ray analysis; EPR spectroscopy; Thermogravimetric analysis

1. Introduction

Hydrazone ligands are condensation products of carbonyl compounds with hydrazine or its alkyl and acyl derivatives. They are known for their versatile biological activities which, in some cases, may be enhanced by coordination with metal ions [1]. Some complexes with hydrazone type ligands show catalytic activity [2], while some polynuclear hydrazone complexes can serve as molecular-based information storage devices [3].

---

*Corresponding author. Email: tamarat@chem.bg.ac.rs

Hydrazones that contain a carbonyl oxygen (O_{hyd}) can be obtained from various hydrazides and carbonyl compounds. If a carbonyl group is directly bound to a hydrazine moiety, then O_{hyd} has a strong coordination tendency. This was previously shown by a Cambridge Structural Database (CSD) [4] survey for hydrazone ligands derived from 2-acetylpyridine (ap) and 2,6-diacetylpyridine (dap) [5], where coordination to O_{hyd} was observed in more than 90% of all the complexes with this ligand type. In *N*-heteroaromatic hydrazones derived from ethyl hydrazinoacetate hydrochloride (haOEt·HCl) as hydrazine derivatives, which were introduced earlier [5–9], the carbonyl group is not part of a hydrazide, but an ester (scheme 1). Consequently, the hydrazinic NH proton becomes less acidic, thus hydrazones derived from haOEt·HCl can coordinate in a neutral form [5–9], which is the case for Cu(II) complexes with *in situ* obtained ligands fphaOEt, aphaOEt, qahaOEt, and dap(haOMe)$_2$ (see scheme 1) [6, 7]. The ester oxygens do not coordinate to the metal in any of these complexes, despite the fact that a stable 6-membered chelate ring may be formed. The same is observed for Cd(II) complexes with aphaOEt and dapha(OEt)$_2$ [5], and Pd(II) and Pt(II) complexes with monohydrazone ligands [8, 9]. Coordination of the ligands in mono-ionic form is observed only when hydrolysis of an ester part of the ligands takes place [8], like in Co(III) and Zn(II) complexes with tridentate aphaOH ligand (see scheme 1). A deprotonated carboxyl coordinates to the metal center via an oxygen (O_{carbox}), in addition to coordination of pyridine and imine nitrogen (N_{py} and N_{im}, respectively).

The fact that complexes of fphaOEt, aphaOEt, qahaOEt, dap(haOMe)$_2$, and dap(haOEt)$_2$ ligands were easily obtained by *in situ* reactions of haOEt·HCl with metal salts and corresponding carbonyl compounds, while complexes with the hydrolyzed form of the ligands were obtained as unexpected products, opened a possibility for investigation of specific reaction conditions towards formation of compounds with the hydrolyzed form of the ligands. Ester hydrolysis occurs during formation of metal organic frameworks by hydrothermal synthesis [10]. Also, syntheses of desired complexes can be done by direct reaction of the hydrolyzed form of the ligands and corresponding metal salts in an appropriate solvent. This conventional direct approach implies three steps: synthesis of the ligands, their hydrolysis and afterwards coordination to metal ions. Template synthesis of complexes via *in situ* hydrolysis has two benefits: (1) higher yield of desired complexes; (2) it is not time and reagent consuming. In this work, one pot reaction conditions towards complex compounds with aphaOH were investigated. Structural characterization and

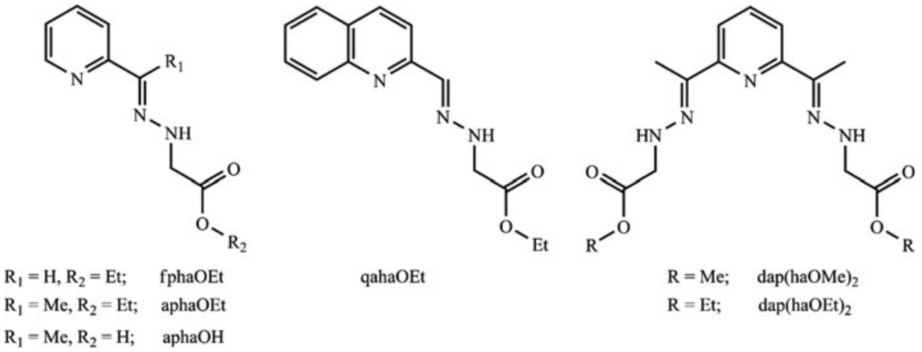

Scheme 1. *N*-heteroaromatic hydrazones derived from (haOEt·HCl).

investigation of thermal stabilities of two compounds with aphaOH, [Cu(aphaO)Cl] (**1**) and $[Zn_2(aphaO)_2Cl_2]$ (**2**) are discussed.

2. Experimental

2.1. *General remarks*

2-Acetylpyridine (99+%) and $CuCl_2{\cdot}2H_2O$ (p.a.) were obtained from Acros Organics, while (haOEt·HCl) (97%) and $Zn(AcO)_2{\cdot}2H_2O$ (p.a.) were obtained from Fluka. Solvents (ethanol 96%, diethyl ether, and acetonitrile 99.5%) were used without purification, except for absolute ethanol, which was obtained by standard methods. Elemental analyses (C, H, N) were performed by standard micro-methods using the ELEMENTAR Vario ELIII C.H. N.S=O analyzer. Infrared (IR) spectra were recorded on a Thermo Scientific Nicolet 6700 FT-IR spectrophotometer by the Attenuated Total Reflection (ATR) in the region $4000-400\,cm^{-1}$. Molar conductivity measurements were performed at ambient temperature on the Crison Multimeter MM41. The 1-D NMR spectra of DMSO-d_6 solutions of the Zn (II) complex (for labeling see figure 1) were obtained using a Bruker Avance 500 instrument equipped with a broad-band direct probe (^{1}H at 500 MHz, ^{13}C at 125.8 MHz). The 2-D NOESY spectrum of the complex was performed on the same instrument, with 8 scans per t1-increment and mixing time of 0.8 s. All spectra were measured at 296 K. Chemical shifts are given on δ scale relative to tetramethylsilane as an internal standard for ^{1}H and ^{13}C. The magnetic measurement of the Cu(II) complex was performed at 304 K by the Evans' method using a MSB-MK1 balance (Sherwood Scientific Ltd.) with $Hg[Co(SCN)_4]$ as a calibrant. Diamagnetic corrections were calculated from Pascal's constants. Continuous wave EPR experiments were performed at ambient temperature on a home-made spectrometer (Laboratory for EPR spectroscopy, Jožef Stefan Institute, Ljubljana, Slovenia). A Larmor frequency of 9.38 GHz (X-band) was used. Electron spray ionization

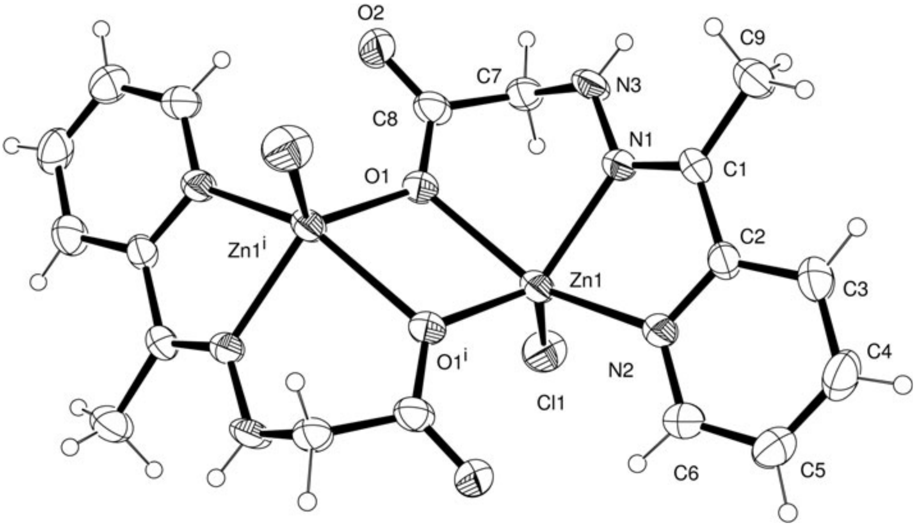

Figure 1. Molecular structure of **2**. The ellipsoids are drawn at 50% probability level, hydrogens at arbitrary size. Equivalent atoms are generated by transformation $-x+1$, $-y$, $-z+1$.

mass spectrum (ESI-MS) of the copper(II) complex was recorded on a Agilent Technologies 6210-1210 TOF-LC-ESI-MS instrument using a methanol/DMSO (7 : 3) solvent mixture. The mass spectrometer was operated in the positive ion mode.

2.2. *Preparation of [Cu(aphaO)Cl] (1)*

The solution of haOEt·HCl (0.15 g, 1.0 mM) and ap (0.12 g, 1.0 mM) in a MeCN/H_2O mixture (20 mL/5 mL) was heated with stirring until the temperature reached 313 K, followed by addition of $CuCl_2 \cdot 2H_2O$ (0.16 g, 0.94 mM). The reaction mixture was refluxed for 30 min and cooled to ambient temperature. Green crystals of **1** were obtained from the mother liquor, filtered off and washed with ether. Yield: 0.19 g (58.8%). Anal. Calcd for $C_9H_{10}ClCuN_3O_2$ (%): C, 37.12; H, 3.46; N, 14.43. Found: C, 36.91; H, 3.67; N, 14.47. IR (ATR, cm^{-1}): 3243 (m), ν(N–H); 1610 (vs. br), ν_{as}(COO) and ν(C=N); 1374 (s), ν_s(COO); 1023 (m), ν(N–N); 650 (w), (pyridine, in plane); 478 (w), (pyridine, out of plane). Λ_M (1×10^{-3} M, DMF): 19.5 $\Omega^{-1} cm^2 M^{-1}$. μ (304 K) = 1.91 μB. ESI-MS: $[M–Cl +DMSO]^+$ ($C_{11}H_{16}N_3O_3SCu$) Calcd *m/z* 333.0208, found 333.0216.

2.3. *Preparation of [Zn₂(aphaO)₂Cl₂] (2)*

A warm solution of ap (0.12 g, 1.0 mM) and haOEt·HCl (0.15 g, 1.0 mM) in absolute ethanol (10 mL) was added to a warm solution of $Zn(AcO)_2 \cdot 2H_2O$ (0.22 g, 1.0 mM) in absolute ethanol (10 mL). The reaction mixture was refluxed for 1 h and cooled to ambient temperature. After two days white crystals of **2** formed were filtered from the mother liquor and washed with ether. Yield 0.20 g (68.2%). Anal. Calcd for $C_{18}H_{20}Cl_2N_6O_4Zn_2$ (%): C, 36.89; H, 3.44; N, 14.34. Found: C, 36.81; H, 3.41; N, 14.35. IR (ATR, cm^{-1}): 3235 (m), ν(N–H); 1646 (vs), ν_{as}(COO) and ν(C=N); 1372 (s), ν_s(COO); 670 (w), (pyridine, in plane); 490 (w), (pyridine, out of plane). ^1H NMR (500 MHz, DMSO-d_6): δ = 2.23 (s, 3H, H–C9), 3.73 (d, 2H, H–C7), 7.55 (br t, 1H, H–N3), 7.84 (d, 1H, H–C3), 8.10 (ovlp, m, 2H, H–C4, and H–C5), 8.49 (br, m, 1H, H–C6). ^{13}C NMR (125.8 MHz, DMSO-d_6): δ = 11.3 (C9), 53.0 (C7), 121.1 (C3), 124.6 (C5), 137.0 (C4), 141.1 (C6), 148.8 (C2), 150.0 (C1), 173.1 (C8). Λ_M (1×10^{-3} M, H_2O): 55.2 $\Omega^{-1} cm^2 M^{-1}$. IR and NMR spectroscopic data, as well as molar conductivity measurements are in agreement with the data previously published [8].

2.4. *X-ray crystallography*

Although **1** was obtained as crystalline material, no crystals suitable for single-crystal X-ray diffraction analysis (XRD) could be found. The unit cell parameters of **1** were determined at ambient temperature from powder X-ray diffraction data obtained by employing a HUBER G670 imaging-plate Guinier camera equipped with a Ge monochromator and Co Kα_1 radiation (λ = 1.788965 Å). LaB_6 (a = 4.15692(1) Å) was used as internal standard.

A single crystal of **2** was selected and mounted on a glass fiber. Diffraction data were collected using an Oxford Diffraction KM4 four-circle goniometer equipped with a Sapphire CCD detector. The crystal to detector distance was 45.0 mm and graphite monochromated Mo Kα (λ = 0.71073 Å) radiation was used for the experiments. The data were reduced using CrysAlisPRO [11]. A semi-empirical absorption-correction based upon the intensities of equivalent reflections was applied, and the data were corrected for

Lorentz, polarization, and background effects. Scattering curves for neutral atoms, together with anomalous dispersion corrections, were taken from the International Tables for Crystallography [12]. The structure was solved by direct methods using the Sir97 program [13] and refined by full-matrix least-squares procedures on F^2 using SHELXS-97 and SHELXL-97 [14] as implemented in the WinGX program suite [15]. The non-H atoms were refined anisotropically. Positions of hydrogens were found from inspection of the difference Fourier maps. At the final stage of refinement, hydrogens from methyl were positioned geometrically (C–H = 0.96 Å) and refined using a riding model with fixed isotropic displacement parameters. Analysis of the crystal geometry was performed by use of the Cambridge Crystallographic Data Center packages [16]. Crystallographic data and refinement parameters are listed in table 1. Figures representing the molecular structure were made using ORTEP-3 [17] and PLATON [18].

2.5. *Thermal analysis*

A coupled TG-MS system was used to study gaseous species evolved during dynamic thermal decomposition (or fragmentation) processes. Thermogravimetric measurements were carried out on a NETZSCH STA409 CD combined with a quadruple mass spectrometer system, QMG422, incorporated in an Argon filled glove-box. The samples were heated to 1073 K under argon at 10 K/min followed by immediate cooling to ambient temperature. Mass spectra were recorded over the whole temperature range. The resulting products were analyzed by powder X-ray diffraction. Long-term annealing (120 h) at 1073 K was performed for both compounds to determine the final products of thermal

Table 1. Crystallographic data and crystal structure refinement details for **2**.

Empirical formula	$C_9H_{10}ClN_3O_2Zn$
Formula weight (g/M)	293.02
Wavelength (Å)	0.71073
Temperature (K)	293(2)
Crystal system	Triclinic
Space group	$P\bar{1}$ (No. 2)
a (Å)	7.9449(7)
b (Å)	8.8623(8)
c (Å)	9.4347(7)
α (°)	69.711(7)
β (°)	71.303(7)
γ (°)	64.926(9)
V (Å^3)	552.45(8)
Z	2
ρ_{calc} (g cm^{-3})	1.761
μ (mm^{-1})	2.451
F(0 0 0)	296
θ_{min}–θ_{max} (°)	3.1–28.9
Refl. collected/unique [R_{int}]	3618/1937(0.030)
Data/restraints/parameters	1937/0/174
Goodness-of-fit on F^2	1.075
R indices (all data)	$R_1 = 0.0324$ $wR_2 = 0.0664$
Final R indices ($I > 2\sigma(I)$)	$R_1 = 0.0283$ $wR_2 = 0.0639$
Largest diff. peak/hole ($e \cdot$Å^{-3})	0.28/−0.26

decomposition. For the thermal annealing experiments, samples were placed in glassy carbon crucibles thereafter enclosed in quartz glass reactors, with connections to an argon supply and relief pressure valve, under flowing argon. The complete reaction setup was thereafter annealed under constant argon flow using one-zone vertical tube furnace. The following heating and cooling procedures were applied: 298 K/8 h/ → 1073 K (const. temperature for 120 h) → 298 K/8 h/. The resulting products were analyzed by means of powder X-ray diffraction.

3. Results and discussion

3.1. *Synthetic aspects*

To obtain a Cu(II) complex with aphaOEt, a template reaction between ap and haOEt·HCl with $CuCl_2·2H_2O$ in ethanol was previously performed [6]. $[CuCl_2(aphaOEt)]$ was obtained as a green crystalline material, which was structurally characterized by a single crystal XRD. In the present work a way to obtain the Cu(II) complex with aphaOH, which is the hydrolyzed form of aphaOEt, by *in situ* reaction was investigated. In order to obtain the desired Cu(II) complex, starting from the same reactants as in the synthesis of $[CuCl_2(aphaOEt)]$, several mixtures of solvents were used. A higher content of water in the reaction mixture increases the crystallization time and, in some cases, even disabled the condensation reaction. The solvent mixture $MeCN:H_2O$ (4 : 1 *v*/*v*) was found to be most suitable, and its use yielded a green polycrystalline compound 24 h after the reaction. Results of the elemental analysis suggested that the Cu : Cl : aphaO molar ratio was 1 : 1 : 1. The ESI-MS spectrum of the complex was recorded in DMSO/methanol (3 : 7). The highest ($m/z = 333$) peak corresponds to $[M–Cl+DMSO]^+$ (exhibiting the appropriate isotope pattern), as the result of DMSO for chloride substitution in the parent complex. The value of the magnetic moment at ambient temperature corresponds to the spin only case, indicating that a neutral, mononuclear compound was obtained (scheme 2). Its composition is in

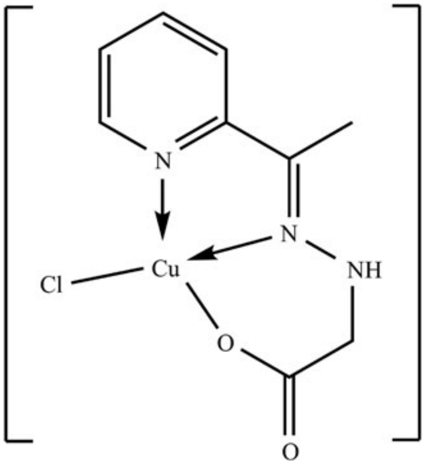

Scheme 2. Proposed model of the molecular structure of [Cu(aphaO)Cl] (1).

accord with the conductivity measurement, IR spectroscopy and observed green color of the complex. Mononuclear compounds with similar ligands are green, such as $[CuCl_2(aphaOEt)]$ and $[CuCl_2(fphaOEt)]$, while the binuclear complex $[Cu_2Cl_4(qahaOEt)_2]$ is brown [6]. Under the same reaction conditions, replacement of ap with aldehydes fp and qa did not result in hydrolysis reactions, thus Cu(II) complexes with the hydrolyzed forms of fphaOEt and qahaOEt were not obtained.

For Zn(II), a polycrystalline complex with the hydrolyzed aphaOEt was previously obtained [8]. The complex was characterized by NMR (^{1}H and ^{13}C) and IR spectroscopy, elemental analysis and molar conductivity. To obtain the Zn(II) complex with aphaOEt and prevent hydrolysis, 96% ethanol was replaced with absolute ethanol, while the molar ratio of all reactants was 1 : 1 : 1. In this reaction, a clear solution was obtained, and after several days, a crystalline product suitable for single-crystal XRD was isolated. Spectral data, elemental analysis, and molar conductivity measurements were consistent with data previously obtained for the polycrystalline Zn(II) compound with the mono-ionic form of aphaOH [8]. A very small amount of water, present in the starting salt $Zn(AcO)_2 \cdot 2H_2O$, was enough to cause hydrolysis. In another attempt to prepare the desired Zn(II) complex with aphaOEt ligand, the starting acetate was replaced by anhydrous $ZnCl_2$. The presence of only haOEt·HCl and ap in the reaction mixture, after reflux with $ZnCl_2$ in absolute ethanol or acetonitrile, was proven by thin layer chromatography [silica gel, ethanol-CH_2Cl_2 (7 : 3, *v*/*v*)]. The presence of acetate in the reaction mixture is needed for the condensation reaction to take place, since acetate is a stronger base than chloride and deprotonates haOEt·HCl.

3.2. *EPR spectroscopy*

To obtain more information about the coordination environment of Cu(II) in **1**, continuous wave EPR experiments were performed at ambient temperature. Line shape simulations for Cu(II) ($S = 1/2$) yielded $g_x = 2.041(5)$, $g_y = 2.061(5)$, and $g_z = 2.254(5)$. The shape of the obtained spectrum was characteristic for axial symmetry and consistent with a tetragonal geometry around Cu(II). The spectrum showed no obvious hyperfine splitting, probably due to weak spin-spin interactions. The effective magnetic moment per Cu(II) ion obtained from EPR measurements is $1.9\,\mu_B$, which is in agreement with the value obtained from magnetic measurements and the expected value from the literature [19].

3.3. *Structure determination*

Due to the poor quality of the crystals, the crystal structure of **1** remains unknown. However, the unit cell parameters and the space group were determined from the results of powder X-ray diffraction. Compound **1** crystallizes in triclinic space group $P\bar{1}$ with the following lattice parameters: $a = 8.234(9)$ Å, $b = 9.123(10)$ Å, $c = 10.057(10)$ Å, $\alpha = 64.11(8)°$, $\beta = 76.13(9)°$, $\gamma = 80.62(16)°$. The solution of the crystal structure of **1** from powder X-ray diffraction data, somewhat complex due to the presence of light atoms in the structure, is in progress.

An ORTEP drawing of binuclear $[Zn_2(aphaO)_2Cl_2]$ (**2**) is depicted in figure 1, while selected bond distances and angles within this complex are given in table 2. The complex lies around an inversion center giving rise to a centrosymmetric dimer. In the coordination sphere of **2**, the mono-deprotonated ligand is coordinated via N_{py} and N_{im}, while carboxylate oxygens bridge metal centers. The fifth coordination site is occupied by a chloride,

Table 2. Selected bond distances (Å) and angles (°) for **2**.

Zn(1)–N(1)	2.130(2)	C(1)–N(1)	1.292(3)
Zn(1)–N(2)	2.131(2)	N(1)–N(3)	1.356(3)
Zn(1)–O(1)	2.2924(18)	N(3)–C(7)	1.454(4)
Zn(1)–O(1)^i	1.9963(18)	C(7)–C(8)	1.513(4)
Zn(1)–Cl(1)	2.2245(8)	C(8)–O(2)	1.220(3)
O(1)^i–Zn(1)–N(1)	130.06(8)	O(1)^i–Zn(1)–O(1)	72.49(7)
N(1)–Zn(1)–N(2)	75.95(8)	O(1)–Zn(1)–N(1)	84.23(7)
O(1)^i–Zn(1)–Cl(1)	113.86(6)	O(1)–Zn(1)–N(2)	151.60(8)
N(1)–Zn(1)–Cl(1)	113.22(6)	O(1)–Zn(1)–Cl(1)	99.66(5)
N(2)–Zn(1)–Cl(1)	106.72(6)	Zn(1)^i–O(1)–Zn(1)	107.51(7)

$^i = -x+1,\ -y,\ -z+1$.

thus the complex is neutral and the coordination number of each Zn(II) is five. The overall geometry of **2** may be described as distorted square pyramidal, since the value for the respective angular structural parameter τ is 0.36 [20]. Heavy distortion of the geometry is further supported by significant displacement of Zn(1) from the mean basal plane [O(1)N(1)N(2)O(1)^i] at 0.6701(3) Å. Due to tridentate coordination of the ligand and formation of binuclear species via carboxylate oxygen bridges, one five-, one six- and one four-membered chelate rings are formed. The pyridine ring and the five-membered chelate ring are almost planar (maximum deviation from the average ring skeleton excluding the metal is 0.1 Å and the angle between the mean planes defined by the fused pyridine ring and the five-membered chelate ring including the metal is 5.6°). Despite the fact that the bond distance range/average is higher than 25%, the results of Cremer and Pople's ring puckering analysis [21] showed that the six-membered chelate ring could be described in a boat conformation [Zn(1)–O(1)–C(8)–C(7)–N(3)–N(1): $Q_T = 0.774$ Å, $\varphi_2 = 183.0°$, $\theta_2 = 82.5°$]. The Zn–(μ-O$_{\text{carbox}}$)$_2$–Zn skeleton exhibits rhombohedral geometry [Zn(1)···Zn(1)^i = 3.463 Å and O(1)···O(1)^i = 2.547 Å]. The Zn(1)–Zn(1)^i distance is similar to metal–metal separations observed in zinc complexes with (μ-O$_{\text{carbox}}$)$_2$ bridges (3.11–3.50 Å) [22]. The Zn–O bond lengths in **2** are comparable to those found in similar zinc(II) complexes with Zn–(μ-O$_{\text{carbox})2}$–Zn bridges [22].

The crystal packing is dominated by intermolecular hydrogen bonds between NH and noncoordinated carbonyl oxygens that give rise to infinite 1-D chains along [1 $\bar{1}$ 0] direction [N3–H···O2 (2–*x*, –1–*y*, 1–*z*) = 2.967(4) Å, N–H···O = 161(3)°]. Intermolecular π–π interactions are also present in this crystal structure. The centroid-centroid distance of stacked pyridine rings is 3.794 Å, while the corresponding displacement angle is 23.79° in accord with a shift of 1.53 Å, thus indicating almost perfect face-to-face alignment [23]. The stacking interactions between neighboring pyridine fragments expand 1-D chains formed by hydrogen bonding into 2-D supramolecular layers parallel to (1 1 0). Finally, these 2-D layers are further interlinked into a 3-D framework (figure 2) by intermolecular C–H···Cl [C5–H5···Cl1 (1–*x*, 1–*y*, –*z*) = 3.754 Å, C–H···Cl = 175.02°] hydrogen bonds.

3.4. *Thermal stability*

In the thermograms of **1** and **2** (Supplementary material), no mass loss is observed up to organic decomposition above 433 K (for **1**) and 513 K (for **2**), which means that the title compounds do not contain coordinated or crystalline water.

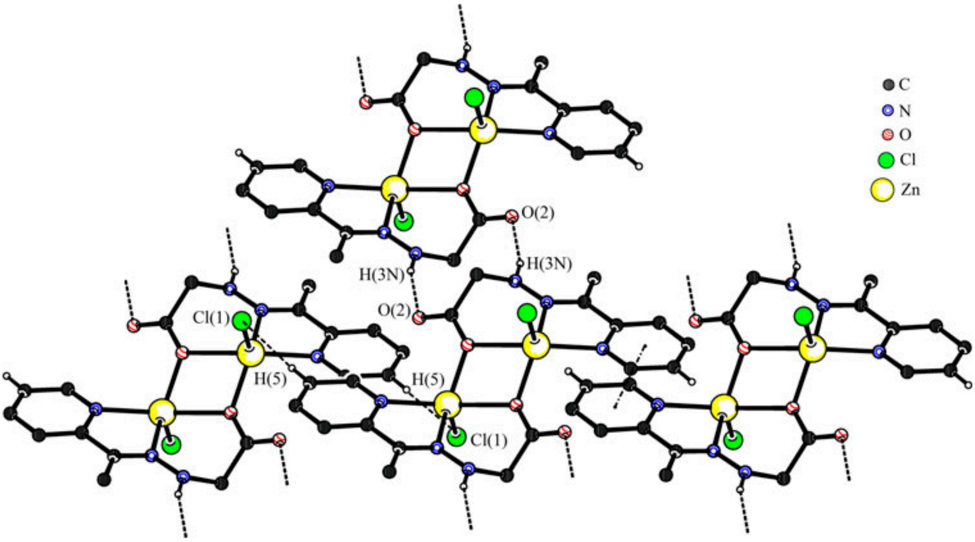

Figure 2. 3-D framework of **2** formed by NH···O and CH···Cl hydrogen bonds (denoted by dashed lines), as well as π-π interactions (denoted by dash-dot line). Hydrogens, except those involved in hydrogen bonding, are omitted for clarity. View direction is parallel to [0 1 0].

Thermal decomposition of both compounds proceeds in four stages and for **2** is not complete in the temperature range from 298 to 1073 K. The observed mass losses in these four stages are presented in table 3. However, a decomposition mechanism for both complexes cannot be proposed by a simple analysis of the mass losses. This indicates that simultaneous decomposition processes take place, which is further supported by analysis of the mass spectra recorded during all four stages.

Data obtained from the MS suggest that thermal degradation of both complexes starts with a decarboxylation process. The most abundant fragment in the mass spectra recorded during the first decomposition stage of both compounds was at a *m/z* value of 44 (with satellites at 45 and 46) originating from CO_2. Also, at the end of the first stage, less intense peaks at 106 (py-CH_2CH_3) and 117–123 (py-$CNCH_n$, $n \leqslant 6$) are observed with their decomposition fragments with lower *m/z* values. The same fragments were observed in mass spectra at the end of the second decomposition stage. At the end of the third stage, the intensities of the signals below $m/z = 50$ are much larger than those in the higher *m/z* region, indicating further decomposition of larger organic fragments. During the last stage of decomposition, the fragments in the higher *m/z* region slowly vanish, while the intensity

Table 3. Thermal decomposition stages for **1** and **2**. Temperature ranges and corresponding mass losses.

	Compound **1**	Compound **2**
Decomposition stage I (K)	433–483	513–553
Observed mass loss (wt.%)	22.02	19.40
Decomposition stage II (K)	483–533	553–643
Observed mass loss (wt.%)	8.38	7.10
Decomposition stage III (K)	533–683	643–773
Observed mass loss (wt.%)	20.33	5.15
Decomposition stage IV (K)	683–1073	673–1073
Observed mass loss (wt.%)	9.41	31.77

of those in the lower *m/z* region increased. The total mass loss during thermal decomposition in the studied temperature region was ~60 wt.% for **1** and ~63 wt.% for **2**.

Powder X-ray diagram of the resulting product for **1** (Supplementary material) indicated a mixture of amorphous and crystalline materials. Several sharp intense lines were observed and identified as carbon, earlier named *n*-diamond [24]. In this crystal structure, six formula units are present in the rhombohedral unit cell with lattice parameters $a = b = 2.5321$ Å and $c = 6.2023$ Å, space group $R3m$ (No. 160). This observation was later confirmed by powder X-ray diffraction data of the resulting product from long term annealing experiments of the same starting material.

The powder X-ray diagram of the resulting solid after decomposition of **2** indicated only amorphous material. In the powder X-ray diagram of the resulting product from long-term annealing experiments of the same starting material, a new modification of zinc oxide, ZnO, may be assigned, next to another phase with unknown crystal structure (Supplementary material). Two sets of peaks can be distinguished, a set of sharp and narrow peaks and a set of broad peaks. All sharp peaks can be indexed on the basis of the $Nb_{0.92}S$ [25] structure type [$P6_3mc$ space group (No. 186)], with lattice parameters $a = b = 5.8021(20)$ Å and $c = 5.6651(21)$ Å. ZnO is the first oxide compound adopting this structure type, next to a few sulfide and nitride compounds, *that is*, δ-MoN [26]. Due to the presence of a second phase with an unknown crystal structure in the resulting product, the structure of the new zinc oxide could not be precisely refined.

In the thermal decomposition of **1** and **2,** only the first two decomposition stages can be compared. According to the mass spectra, the most intense process in the first stage is decarboxylation of the ligand. In the second stage, besides decarboxylation, loss of 2-ap imine fragment dominates. Although in the later stages further decomposition of organic fragments takes place, one big difference has to be noted. In the product after thermal decomposition of **1,** no compound containing copper could be identified.

4. Conclusions

The copper(II) complex with the aphaOEt ligand was previously synthesized starting from ap, haOEt·HCl and $CuCl_2$ in an ethanolic solution. In the present study, a variety of reaction conditions towards formation of the Cu(II) complex with the hydrolyzed form of the aphaOEt ligand was investigated. It was found that mixture of MeCN and H_2O (4:1 v/v) is most suitable for one pot formation of **1**. Tridentate coordination (N_{py},N_{im},O_{carbox}) of the mono-anionic form of aphaOH is postulated, while the fourth coordination site in the inner sphere of **1** is occupied by a chloride. Attempts to synthesize Cu(II) complexes with the hydrolyzed form of the corresponding ligands by *in situ* reactions of haOEt·HCl with *N*-heteroaromatic aldehydes (fp and qa) remained unsuccessful. This may indicate that the type of carbonyl compound plays a significant role in the synthesis, next to impact of the solvent.

Regardless of experimental conditions such as choice of solvent, molar ratio of reactants, presence of water in the reaction mixture, the Zn(II) complex **2** with the hydrolyzed form of aphaOEt is exclusively formed. It was previously postulated that a mononuclear tetrahedral complex was obtained, but in the present study, a single crystal XRD revealed the binuclear nature of this compound in the solid state. In the inner sphere of **2**, chloride is coordinated to Zn(II). The ligand is coordinated in the mono-anionic form via N_{py} and

N_{im}, while the carboxylate oxygen is a double donor, bridging two metal centers. This coordination of carboxylate oxygen to Zn(II) is rare, as shown from a survey of Cambridge Structural Database (CSD). Overall geometry of both metal centers in **2** can be described as a distorted square pyramid. The crystal packing of **2** is dominated by intermolecular hydrogen bonds and π–π interactions. In the 2-D NOESY spectrum of the Zn(II) complex, there is no correlation signal between protons that are spatially close in the molecular structure of the complex in the solid state (CH_2 from one ligand and aromatic C6 proton from the second one). Since a signal can be observed only if the distance is smaller than 5 Å, and the distance between the above mentioned protons is close to the limit, it remains unknown if the geometry and nuclearity of the Zn(II) complex is preserved in solution.

Thermal decompositions of **1** and **2** occur via four stages. Both complexes show moderate thermal stability, with the Zn(II) complex showing slightly higher thermal stability.

Supplementary material

CCDC 875363 contains the supplementary crystallographic data for **2**. These data can be obtained free of charge via http://www.ccdc.cam.ac.uk/conts/retrieving.html, or from the Cambridge Crystallographic Data Center, 12 Union Road, Cambridge CB2 1EZ, UK; Fax: (+44) 1223-336-033; or E-mail: deposit@ccdc.cam.ac.uk. Supplementary data associated with this article can be found in the online version at doi:10.1080/00958972.2013.786052.

Acknowledgments

The authors would like to acknowledge the help of Dr S. Hoffmann and S. Scharsach from MPI CPfS in Dresden with the TG-MS measurements and data analyses, and Dr H. Borrmann for his help, guidance and support. N.F., M.J. and T.T. gratefully acknowledge the financial support by the Max Planck Society and the opportunity to work at MPI in Dresden, where a part of this work was done. This work was supported by the Ministry of Education and Science of the Republic of Serbia (Grant 172055).

References

[1] (a) M.R. Maurya, R. Mannar, S. Agarwal, M. Abid, A. Azam, C. Bader, M. Ebel, D. Rehder. *Dalton Trans.*, 937 (2006), and references therein; (b) M. Carcelli, P. Mazza, C. Pelizzi, G. Pelizzi, F. Zani. *J. Inorg. Biochem.*, **57**, 43 (1995), and references therein.

[2] (a) C. Amort, M. Malaun, A. Krajete, H. Kopacka, K. Wurst, M. Christ, D. Lilge, M.O. Kristen, B. Bildstein. *Appl. Organomet. Chem.*, **16**, 506 (2002); (b) P. Liu, W. Zhang, R. He. *Appl. Organomet. Chem.*, **23**, 135 (2009).

[3] K.V. Shuvaev, L.N. Dawe, L.K. Thompson. *Dalton Trans.*, 4768 (2010), and references therein.

[4] F.H. Allen. *Acta Crystallogr.*, **B58**, 380 (2002).

[5] N. Filipović, T. Todorović, D. Radanović, V. Divjaković, R. Marković, I. Pajić, K. Anđelković. *Polyhedron*, **31**, 19 (2012).

[6] N. Filipović, H. Borrmann, T. Todorović, M. Borna, V. Spasojević, D. Sladić, I. Novaković, K. Anđelković. *Inorg. Chim. Acta*, **362**, 1996 (2009).

[7] K. Anđelković, R. Tellgren, S. Niketić, D. Sladić, D. Poleti. *J. Chem. Crystallogr.*, **29**, 575 (1999).

[8] N. Filipović, A. Bacchi, G. Pelizzi, R. Marković, D. Mitić, K. Anđelković. *J. Coord. Chem.*, **58**, 1541 (2005).

[9] N.R. Filipović, T.R. Todorović, D.M. Sladić, I.T. Novaković, D.A. Jeremić, K.K. Anđelković. *Mater. Sci. Forum*, **555**, 423 (2007).

[10] X.-M. Zhang. *Coord. Chem. Rev.*, **249**, 1201 (2005).

[11] Agilent *CrysAlis PRO*, Agilent Technologies, Oxfordshire (2010).

[12] A.J.C. Wilson (Ed.). *International Tables for X-ray Crystallography*, Vol. C, Kluwer Academic Publishers, Dodrecht (1992). Tables used: 6.1.1.4. (pp. 500–502), 4.2.6.8 (pp. 219–222) and 4.2.4.2 (pp. 193–199).

[13] (a) A. Altomare, M.C. Burla, M. Cavalli, G. Cascarano, C. Giacovazzo, A. Gagliardi, A.G. Moliterni, G. Polidori, R. Spagna, *Sir97: A New Program For Solving and Refining Crystal Structures*, University of Bari, Italy (1997); (b) A. Altomare, M.C. Burla, M. Cavalli, G. Cascarano, C. Giacovazzo, A. Gagliardi, A. G.G. Moliterni, G. Polidori, R. Spagna. *J. Appl. Cryst.*, **32**, 115 (1999).

[14] (a) G.M. Sheldrick, *SHELXS-97 and SHELXL-97. Programs for solution and refinement of crystal structures from diffraction data*, University of Göttingen, Germany (1997); (b) G.M. Sheldrick. *Acta Crystallogr.*, **A64**, 112 (2008).

[15] (a) L.J.Farrugia, *WinGX*, University of Glasgow, Scotland (1998); (b) L.J. Farrugia. *J. Appl. Cryst.*, **32**, 837 (1999).

[16] (a) F.H. Allen, O. Kennard, R. Taylor. *Acc. Chem. Res.*, **16**, 146 (1983); (b) I.J. Bruno, J.C. Cole, P.R. Edgington, M. Kessler, C.F. Macrae, P. McCabe, J. Pearson, R. Taylor. *Acta Crystallogr.*, **B58**, 389 (2002).

[17] (a) L.J. Farrugia, *ORTEP-3 for Windows*, University of Glasgow, Scotland (1997); (b) L.J. Farrugia. *J. Appl. Cryst.*, **30**, 565 (1997).

[18] A.L. Spek. *Acta Crystallogr.*, **D65**, 148 (2009).

[19] N.W. Ashcroft, N.D. Mermin, *Solid State Physics*, 1st edn, p. 658, Saunders College, Philadelphia (1976).

[20] (a) The parameter τ [$\tau = (\beta - \alpha)/60°$, where $(\beta - \alpha)$ stands for the difference of in-plane *trans* bond angles] is an index of the degree of trigonality, within the structural continuum between trigonal bipyramidal and square-based pyramidal geometry; (b) A.W. Addison, T.N. Rao, J. Reedijk, J. van Rijn, G.C. Verschoor. *Dalton Trans.*, 1349 (1984).

[21] D. Cremer, J.A. Pople. *J. Am. Chem. Soc.*, **97**, 1354 (1975).

[22] (a) M. Barcelo-Oliver, A. Terron, A. Garcia-Raso, J.J. Fiol, E. Molins, C. Miravitlles. *J. Inorg. Biochem.*, **98**, 1703 (2004); (b) L. La-Sheng, D. Ke-Yang, C. Xiao-Ming, J. Liang-Nian. *Inorg. Chem. Commun.*, **3**, 65 (2000); (c) F. Yaoting, H. Xiankuan, W. Liya, M. Lufang. *J. Coord. Chem.*, **60**, 1619 (2007); (d) A. Grirrane, A. Pastor, E. Alvarez, C. Mealli, A. Ienco, A. Galindo. *Inorg. Chem. Commun.*, **9**, 160 (2006); (e) L.-Y. Wang, Y.-W. Wang, X.-D. Wang, L.-F. Ma. *Jiegou Huaxue (Chin. J. Struct. Chem.)*, **28**, 983 (2009); (f) R. Pandey, M. Yadav, P. Kumar, P.-Z. Li, S.K. Singh, Q. Xu, D.S. Pandey. *Inorg. Chim. Acta*, **376**, 195 (2011).

[23] (a) The displacement was measured by the angle formed between the vector through centroids of respective rings and a vector normal to the ring planes; (b) C. Janiak. *Dalton Trans.*, 3885 (2000).

[24] B. Wen, J. Zhao, T. Li, C. Dong. *New J. Phys.*, **8**, 62 (2006).

[25] F. Kadijk, F. Jellinek. *J. Less-Common Met.*, **19**, 421 (1969).

[26] C.L. Bull, P.F. McMillan, E. Soignard, K. Leinenweber. *J. Solid State Chem.*, **177**, 1488 (2004).